Reconfigurable Ultra-Wide Band See-Through-Wall Imaging Radar System

Yazhou Wang, Yunqiang Yang and Aly E. Fathy
EECS Department, The University of Tennessee, Knoxville, TN, 37996
E-mail: ywang34@utk.edu

Introduction

Previously, we built two separate see-through-wall (STW) imaging radar systems. The systems operated at either a 1 to 3 GHz for lower loss propagation, or an 8 to 10 GHz for higher imaging resolution. It is well known that wall-attenuation increases with frequency, so the image resolution improves at these higher frequencies. Therefore, a compromise is needed between acceptable wall attenuation and an adequate imaging resolution. A 8-10 GHz operation has been recommended in [1] for penetrating drywall to get the best imaging resolution, but a 1-3 GHz was utilized as the optimal frequency band for through brick/concrete wall applications in [2] to minimize the through wall losses.

In this paper, we present in detail a reconfigurable UWB imaging radar system architecture for STW applications used upon various types of building materials. The reconfigurable system, elegantly combining the previously developed two systems, is restructured to work at either a 1-3 GHz or 8-10 GHz frequency band. Depending upon the type of building materials, we will reap the benefits of either a lower traveling loss or better imaging resolution.

8-10 GHz Imaging Radar System

A detailed block diagram of our previously developed 8-10 GHz radar system is outlined in Fig. 1. A 1ns pulse [3] is applied to the system. A carrier frequency of 9 GHz was chosen in order to acquire a high image resolution when penetrating through drywall scenarios. The reconstructed I and Q data are sent to the ADC for sampling using the equivalent time sampling scheme [4]. Next, all the sampling data are sent to a FPGA circuitry for post-processing. Last, the image is recovered via a microwave beam-forming algorithm implemented using a Matlab program [5].

A data acquisition module has been actualized using an off-the-shelf Avnet Xilinx Virtex-4 FPGA board with a Texas Instrument CDC5801 low-jitter clock multiplier/divider, and two MAX108 ADC evaluation boards with a 2.2 GHz analog bandwidth and a 170 MHz maximum sampling rate. The module implements a hybrid sampling (100MS/s real-time rate and 5GS/s equivalent-time rate) scheme. The data acquisition module, including the real-time control scheme, is shown in Fig. 2. The Avnet FPGA board, utilizing FPGA-VHDL coding, provides varying sets of logic control signals, such as SAR array switching and system synchronization. The ADC outputs are 12-bit digital differential signals (LVDS) which represent the digitized pulse value. The digitized output is sent, and stored, in the memory of the FPGA board for further processing.

978-1-4244-3647-7/09/$25.00 ©2009 IEEE

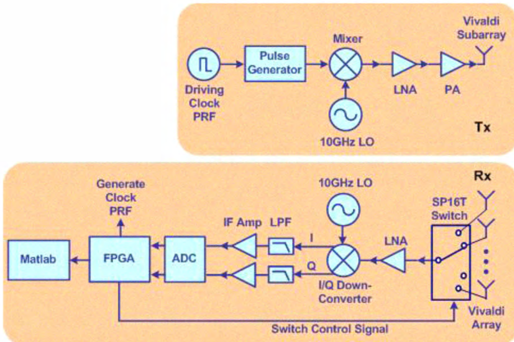

Fig. 1. Detailed block diagram of the 8-10 GHz imaging radar system

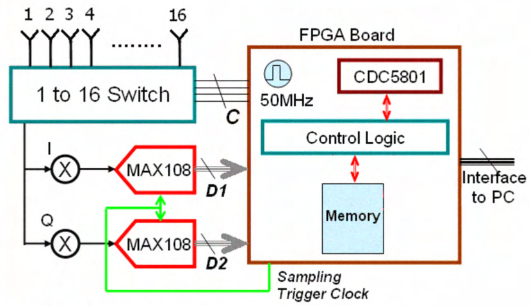

Fig. 2. Detailed diagram of data acquisition and digital control

8-10 GHz System Experiment

An on-site experiment has been conducted to evaluate the performance of the 8-10 GHz STW system. The experiment was conducted in the hallway of an office building. The floor layout of the setup is demonstrated in Fig. 3. A 2-inch plywood panel wall was placed in front of the radar and stationary imaging was tested. The resulting image in Fig. 4 clearly identifies the position of targets. The image also displays the environmental response, including side wall and metal doors.

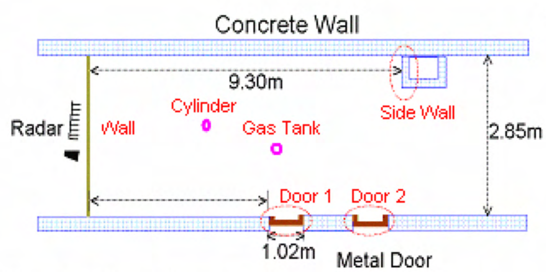

Fig. 3. Floor layout of experimental setup

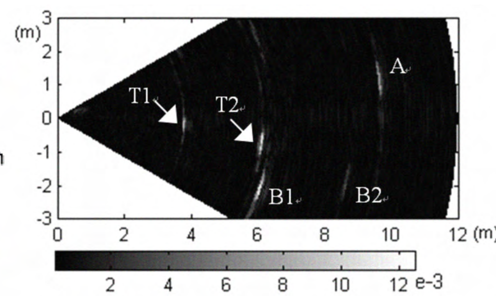

Fig. 4. Image of stationary targets: T1-Cylinder, T2-Gas Tank, A-Side Wall, B1-Door 1, B2-Door 2

Reconfigurable System Architecture

To extend the operation of the previous system to cover both bands, we redesigned the system to offer a wideband operation. The new system is composed of extremely wide band antennas to encompass the entire 1 to 10 GHz frequency range [6], and a set of switches. A detailed block diagram of the proposed reconfigurable imaging radar system is outlined in Fig. 5. The aggregate system can be reconfigured to operate at two different frequency bands using four SPDT switches, two of which are in the transmitting chain and the other two are in the receiving chain. A 10 MHz clock (PRF) generated by the FPGA is used to drive a Gaussian pulse generator [3]. The pulse is then modulated by a carrier signal of either 2 GHz (LO1) or 9 GHz (LO2), which is selected by a SPDT switch1. The modulated signal chosen by the SPDT Switch2 passes through two stages of amplification and is transmitted via a wideband Vivaldi subarray. The wideband power amplifier in the transmitting chain has a 12 dB gain from DC to 10 GHz. Its typical 1dB compression point is 28 dBm; i.e. the maximum output power is approximately 0.63 W.

At the Rx link, the signal received by the wideband Vivaldi array passes through the SP16T switch and then is amplified by a wideband low noise amplifier (LNA) with a 14 dB gain from DC to 10 GHz and a 4 dB noise figure. Next, the signal is selected by a SPDT switch2 prior to being down-converted into I and Q channels by mixing the same carrier signal, as the selected one in up-converter, with the received signal. The I/Q mixer3 (1-3 GHz) and mixer4 (8-10 GHz) employed have a conversion loss of 8dB and 7dB respectively. Then, the recovered I and Q data are opted, filtered and amplified before being sent for post-data processing to retrieve the image, as indicated previously. All the SPDT switches and the SP16T switch are controlled by logic signals generated from the same FPGA.

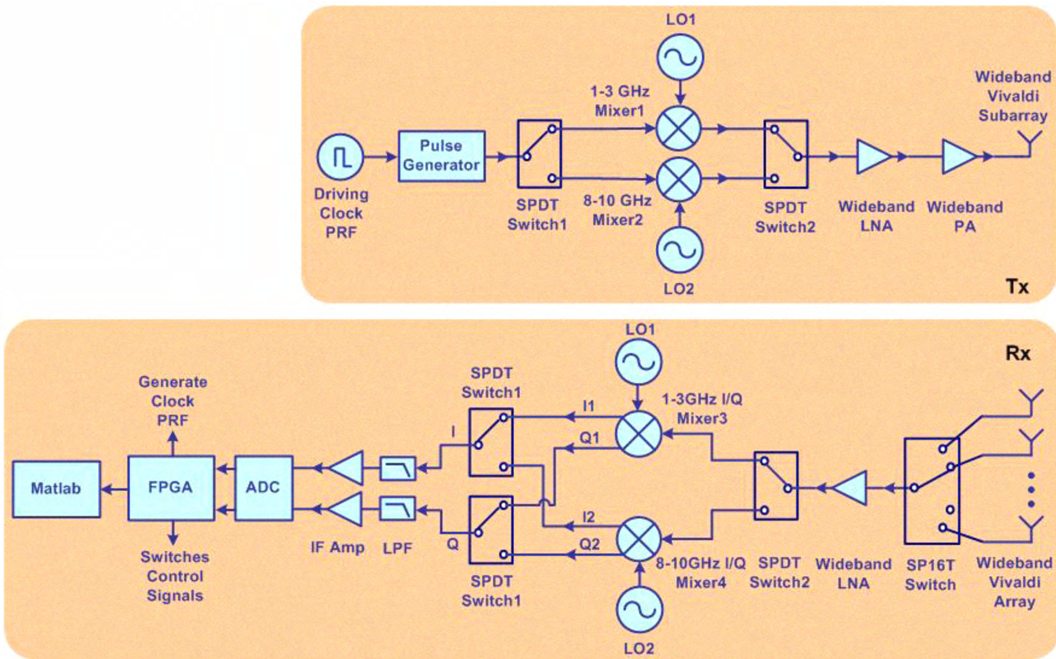

Fig. 5. Detailed block diagram of the reconfigurable imaging radar system

Reconfigurable System Simulation

We have successfully used Agilent Advance Design System (ADS) to simulate our reconfigurable radar system. The pulse applied in the simulation has a width of 1ns, which occupies a 2 GHz bandwidth in the frequency domain. Signal traveling in the air and through-the-wall has been modeled as a combination of delay and attenuation. Normal incidence was assumed in the simulation when signals penetrate through the wall. The system was reconfigured via the SPDT switches to work at either a 1-3 GHz or 8-10 GHz frequency band. Figs. 6 (a) and 7 (a) depict the transmitted and recovered pulse signals when the radar system works at a 1-3 GHz and 8-10 GHz, respectively. Slight distortions and pulse broadening exist in Fig. 6 (a) due to the nonlinear effects from the active devices. The pulse signals modulated by the 2 GHz and 9 GHz carriers are presented in Figs. 6 (b) and 7 (b), respectively. An excellent amplitude envelope is achieved when applying a 9 GHz carrier; however, a small quantity of information may be lost in the modulation when assigning a 2 GHz carrier. To negate this issue, a wider pulse, such as a 2ns pulse, can be applied when the system functions at a 1-3 GHz frequency band.

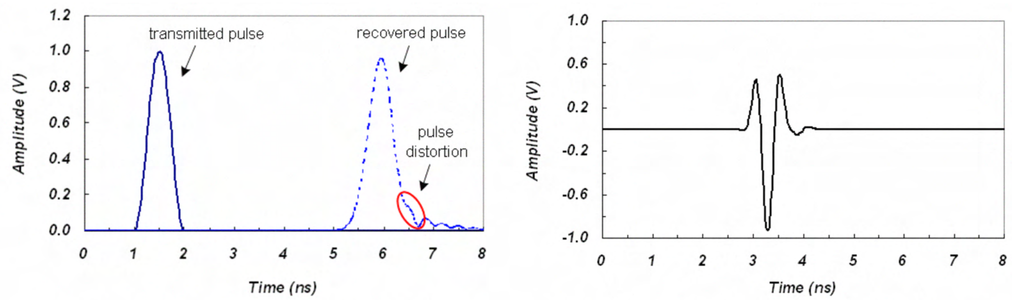

(a) Transmitted and recovered pulses (b) Pulse modulated by a 2 GHz carrier

Fig. 6. Simulation results when the system operates at 1-3 GHz

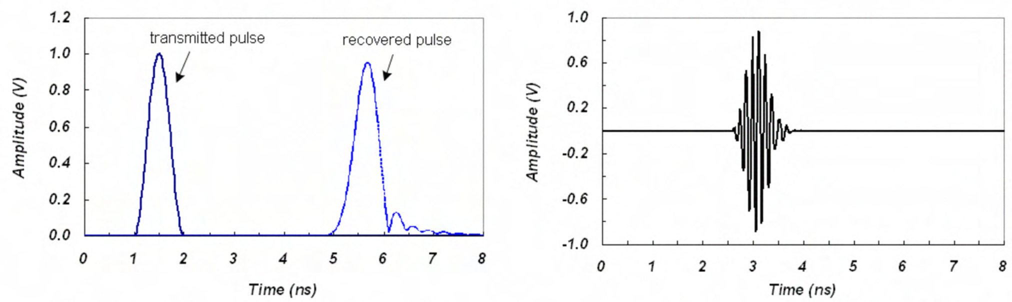

(a) Transmitted and recovered pulses (b) Pulse modulated by a 9 GHz carrier

Fig. 7. Simulation results when the system operates at 8-10 GHz

Conclusion

An 8-10 GHz imaging radar system has been presented, demonstrating excellent experimental results when implementing STW applications on drywall material. As an extension, a reconfigurable ultra-wide band STW radar system is proposed to be employed in conjunction with various types of building materials. The reconfigurable system can be reconfigured using four SPDT switches to operate at either a 1-3 GHz or 8-10 GHz, while utilizing the same ADC and FPGA board. Preliminary results are encouraging and will be presented in detail.

References

[1] Y. Yang and A. E. Fathy, “See-through-wall imaging using ultra wideband short-pulse radar system,” IEEE AP-S Intl. Symp., Vol. 3B, pp. 334-337, July 2005.

[2] Mark Farwell et al., “Sense through the wall system development and design considerations,” Journal of the Franklin Institute, Vol. 345, Issue 6, pp. 570-591, Sep. 2008.

[3] Cemin Zhang and A. E. Fathy, “Reconfigurable Pico-Pulse Generator for UWB Applications,” 2006 IEEE MTT-S Int. Microwave Symp. Dig., pp. 407-410, June 2006.

[4] Mark Kahrs, “50 Years of RF and Microwave Sampling,” IEEE Trans. Microwave Theory & Tech., vol. 51, No. 6, June 2003.

[5] G. Wang, M. G. Amin, and Y. Zhang, “New approach for target locations in the presence of wall ambiguities,” IEEE Trans. on Aero. & Elec. Systems, vol. 42, issue 1, pp. 301-315, Jan 2006.

[6] Y. Wang et al., “Ultra-wideband Vivaldi arrays for see-through-wall imaging radar applications,” submitted to IEEE 2009 AP-S, Jan. 2009.